

# Journal of Visualized Experiments

## Fluorescence-Activated Cell Sorting-Radioligand Treated Tissue (FACS-RTT) to determine the cellular origin of radioactive signal --Manuscript Draft--

<b>Article Type:</b>	Invited Methods Collection - JoVE Produced Video
<b>Manuscript Number:</b>	JoVE62883R2
<b>Full Title:</b>	Fluorescence-Activated Cell Sorting-Radioligand Treated Tissue (FACS-RTT) to determine the cellular origin of radioactive signal
<b>Corresponding Author:</b>	Benjamin Tournier Geneva University Hospitals: Hopitaux Universitaires Geneve geneva, geneva SWITZERLAND
<b>Corresponding Author's Institution:</b>	Geneva University Hospitals: Hopitaux Universitaires Geneve
<b>Corresponding Author E-Mail:</b>	Benjamin.Tournier@hcuge.ch
<b>Order of Authors:</b>	<div>Quentin Amossé</div> <div>Kelly Ceyzériat</div> <div>Stergios Tsartsalis</div> <div>Benjamin Tournier</div> <div>Philippe Millet</div>
<b>Additional Information:</b>	
<b>Question</b>	<b>Response</b>
Please specify the section of the submitted manuscript.	Neuroscience
Please indicate whether this article will be Standard Access or Open Access.	Standard Access (\$1400)
Please indicate the <b>city, state/province, and country</b> where this article will be <b>filmed</b> . Please do not use abbreviations.	Geneva, Geneva, Switzerland
Please confirm that you have read and agree to the terms and conditions of the author license agreement that applies below:	I agree to the <a href="#">Author License Agreement</a>
Please provide any comments to the journal here.	
Please confirm that you have read and agree to the terms and conditions of the video release that applies below:	I agree to the <a href="#">Video Release</a>

**TITLE:**

Fluorescence-Activated Cell Sorting-Radioligand Treated Tissue (FACS-RTT) to Determine the Cellular Origin of Radioactive Signal

**AUTHORS AND AFFILIATIONS:**

Quentin Amossé<sup>1,2</sup>, Kelly Ceyzériat<sup>1,3,4</sup>, Stergios Tsartsalis<sup>1,5</sup>, Benjamin B Tournier<sup>1,2</sup>, Philippe Millet<sup>1,2</sup>

<sup>1</sup>Division of Adult Psychiatry, Department of Psychiatry, University Hospitals of Geneva, Avenue de la Roseraie, 64, 1206 Geneva, Switzerland

<sup>2</sup>Department of Psychiatry, University of Geneva, Geneva, Switzerland

<sup>3</sup>Division of Nuclear medicine and Molecular Imaging, University Hospitals of Geneva, Avenue de la Roseraie, 64, 1206 Geneva, Switzerland

<sup>4</sup>Division of Radiation Oncology, Department of Oncology, University Hospitals of Geneva, Geneva, Switzerland

<sup>5</sup>Department of Brain Sciences, Faculty of Medicine, Imperial College London, London, UK

Email addresses of co-authors:

Quentin Amossé (quentin.amosse@unige.ch)

Kelly Ceyzériat (kelly.ceyzeriat@unige.ch)

Stergios Tsartsalis (stergios.tsartsalis@hcuge.ch)

Benjamin B Tournier (benjamin.tournier@hcuge.ch)

Philippe Millet (philippe.millet@hcuge.ch)

Corresponding author:

Benjamin B Tournier (benjamin.tournier@hcuge.ch)

**KEYWORDS:**

Alzheimer's disease, Fluorescence-Activated Cell Sorting to Radioligand Treated Tissues, TgF344-AD, Positron Emission Tomography/Single Photon Emission Computed Tomography, TSPO, 5HT<sub>2A</sub>R

**SUMMARY:**

Fluorescence-Activated Cell Sorting-Radioligand Treated Tissue (FACS-RTT) is a powerful tool to study the role of the 18 kDa translocator protein or Serotonin 5HT<sub>2A</sub>-receptor expression in Alzheimer's Disease at a cellular scale. This protocol describes the *ex-vivo* application of FACS-RTT in the TgF344-AD rat model.

**ABSTRACT:**

Glial cells probably have a considerable implication in the pathophysiology of neurodegenerative disorders, such as Alzheimer's disease (AD). Their alterations are perhaps associated with a pro-inflammatory state. The TgF344-AD rat strain has been designed to express human APP and human PS1<sub>ΔE9</sub> genes, encoding for amyloid proteins Aβ-40 and Aβ-42 and displays amyloid pathology and cognitive deficits with aging. The TgF344-AD rat model is used in this study to

evaluate the cellular origin of the 18 kDa translocator protein (TSPO, a marker of glial cell activation) binding, and the 5HT<sub>2A</sub>-receptor (5HT<sub>2A</sub>R) serotonin receptor levels that are possibly disrupted in AD. The technique presented here is Fluorescence-Activated Cell Sorting to Radioligand Treated Tissue (FACS-RTT), a quantitative cell-type-specific technique complementary to *in vivo* PET or SPECT or *ex vivo/in vitro* autoradiography techniques. It quantifies the same radiolabeled tracer used prior for imaging, using a  $\gamma$  counter after cytometry cell sorting. This allows determining the cellular origin of the radiolabeled protein with high cellular specificity and sensitivity. For example, studies with FACS-RTT showed that (i) the increase in TSPO binding was associated with microglia in a rat model of lipopolysaccharide (LPS)-induced neuroinflammation, (ii) an increase in TSPO binding at 12- and 18-months was associated with astrocytes first, and then microglia in the TgF344-AD rats compared to wild type (WT) rats, and (iii) the striatal density of 5HT<sub>2A</sub>R decreases in astrocytes at 18 months in the same rat AD model. Interestingly, this technique can be extended to virtually all radiotracers.

## INTRODUCTION:

Neurodegenerative diseases, such as Alzheimer's Disease (AD), are characterized by a neuronal loss associated with increased symptoms. AD, the most common cause of dementia, accounting 60%–70% of cases, affects around 50 million people worldwide<sup>1</sup>. At a neuropathological level, the two major characteristics of AD are the accumulation of extracellular amyloid- $\beta$  (A $\beta$ ) plaques and intracellular Tau neurofibrillary tangles. Glial cell alterations have also been associated with AD<sup>2</sup> and possible disruption of several neurotransmitter systems<sup>3,4</sup>.

The TgF344-AD rat line has been modified to model AD by expressing human APP and PS1 $\Delta$ E9 transgenes, leading to soluble and insoluble A $\beta$ -40 and A $\beta$ -42 expression and amyloid plaque formation<sup>5</sup>. It also presents the accumulation of hyperphosphorylated forms of the Tau protein leading to tauopathy. From the age of 9–24 months, the rats progressively develop the pathological hallmarks of AD and a cognitive impairment<sup>5–9</sup>.

Positron Emission Tomography (PET), Single-Photon Emission computed Tomography (SPECT), and autoradiography are techniques based on the emission and quantification of  $\gamma$  rays. Radiotracers are quantified either *in vivo* (PET and SPECT) or *ex vivo/in vitro* (autoradiography). Those sensitive techniques have contributed to the understanding of mechanisms of several brain diseases, such as AD. Indeed, in terms of neuroinflammation, there are a lot of studies assessing 18 kDa Translocator Protein (TSPO), an *in vivo* neuroinflammation marker, with radiolabeled tracers such as [<sup>11</sup>C]-(R)-PK11195 or [<sup>11</sup>C]PBR28 (for review see<sup>10</sup>). In addition, alterations of neurotransmitter systems have been studied using radiotracers<sup>11–13</sup>.

However, those techniques do not determine the cellular origin of the radioactive signal. This could hamper the interpretation of the biological underpinnings of the alteration in the binding of a radioligand in PET/SPECT. For instance, in the case of TSPO studies of neuroinflammation, understanding whether the increase or decrease of TSPO is due to astrocytic or microglial changes is of paramount importance. The Fluorescence-Activated Cell Sorting to Radioligand Treated Tissue (FACS-RTT) technique was developed to get around these problems, allowing the assessment of radioligand binding in every cell type separately and the quantification of the

target-protein density per cell. This innovative technique is consequently complementary and highly compatible with PET and SPECT imaging.

Here, this technique was applied along two axes: the study of neuroinflammation using TSPO-specific radioligands and assessing the serotonergic system. On the first axis, the aim was to understand the cellular origin of the TSPO signal in response to an acute inflammatory reaction. Therefore, FACS-RTT was used on the brain tissues of rats after the induction of neuroinflammation via a lipopolysaccharide (LPS) injection and following an *in vivo* [<sup>125</sup>I]CLINDE SPECT imaging study. Further, the same imaging and FACS-RTT protocol were applied on 12- and 24-month-old TgF344-AD rats and matching wild-type (WT) rats. The second axis aimed to determine the origin of serotonergic system alterations in this rat model via *ex vivo* 5-HT<sub>2A</sub>R density assessment by cell type.

## PROTOCOL:

All experimental procedures were conducted in agreement with the Ethics Committee for Human and Animal Experimentation of the Canton of Geneva, the Cantonal Commission for Research Ethics (CCER), and the General Direction Of The Health Of The Canton Of Geneva (Switzerland), respectively. Data are reported following Animal Research: Reporting *In-vivo* Experiments (ARRIVE) guidelines.

### 1 SPECT camera preparation and calibration

1.1 Turn on the camera, load the operating software (see **Table of Materials**). Click on the **Home XYZ Stage** button to perform homing.

1.2 Set up the experiment composed of one 10 min scan acquisition. Set the **Step** mode to **Fine** and the **Acquisition** mode to the **Listmode** (to record the entire emission spectrum).

1.3 Set up the bed and ensure that the warming system, breathing sensor, and anesthesia are functional and secure (**Figure 1A–D**). Then, place a phantom (i.e., 2 mL of a known concentration of <sup>125</sup>I in a 2 mL microfuge tube) where the animal's head will be positioned (centered on the area, **Figure 1E**).

1.4 Set the scan area by sliding the cursors for the three dimensions with the help of the three images in the bottom part of the screen. Ensure that the scan volume of the phantom and the animal is the same.

1.5 Start the phantom scan for subsequent calibration with the parameters established in steps 1.2–1.4.

### 2 Workspace setup for SPECT imaging

- 2.1 Clean the workspace with disinfectant virucide and place soft papers on all the surfaces.
- 2.2 Ensure that there is enough isoflurane and oxygen in their respective tanks.
- 2.3 Prepare a 24 G catheter by cutting off the fins of the butterfly catheter to have a clearer view of the rat tail vein.
- 2.4 Coat the catheter by filling it completely with heparin solution (25000 U/mL) after removing the needle. Then, place the needle back in it to avoid blood clot formation following catheter insertion.

### 3 [<sup>125</sup>I]CLINDE radiotracer synthesis

CAUTION: Radioactivity can have sufficient ionizing energy to affect the atoms of the living cells and damage their genetic material (DNA).

- 3.1 Ensure to work in an appropriate environment, authorized for experiments involving radioactivity.

NOTE: Wear the appropriate personal protective equipment (PPE), for radioactivity handling, including finger and body dosimeters. Try to stay at a safe distance from any source of radioactivity.

- 3.2 Incubate 100 µg of tributyltin precursor in 100 µL of acetic acid with sodium iodide (Na<sup>125</sup>I) (see **Table of Materials**) and 5 µL of 37% peracetic acid at 70 °C for 20 min in a thermocycler positioned in a glove box.

- 3.3 Dilute the reaction using 50% acetonitrile (ACN) in water to reach a volume of 500 µL. Inject the 500 µL of the diluted reaction onto a reverse-phase column (see **Table of Materials**).

- 3.4 Isolate the [<sup>125</sup>I]CLINDE with a linear gradient HPLC run from 5%–95% ACN in 7 mM H<sub>3</sub>PO<sub>4</sub> for 10 min. Dilute the isolate in H<sub>2</sub>O to attain a final volume of 10 mL, and then inject the diluted reaction onto a concentration column (see **Table of Materials**).

- 3.5 Elute the [<sup>125</sup>I]CLINDE from the column with 300 µL of absolute ethanol, and then evaporate the ethanol by incubating it in a vacuum centrifuge at RT for 40 min.

- 3.6 Dilute the residue containing the [<sup>125</sup>I]CLINDE in 300 µL of saline to create a stock solution.

- 3.7 After measuring its radioactivity, dilute the stock solution in saline to obtain a solution of 0.037 MBq in 500 µL.

- 3.8 Purify the tracer by HPLC (High-performance liquid chromatography). Determine the elution time using a standard calibration at 450 nm, and isolate the single radioactive peak.

Perform the standard calibration curve using seven standard concentrations of cold (non-radioactive) CLINDE (0.1 µg, 0.5 µg, 0.75 µg, 1 µg, 1.5 µg, 2 µg, and 5 µg in 400 µL of a solution of 50% ACN. Establish the radiochemical purity by measuring a single peak in radio TLC (Thin layer chromatography). Ensure that the purity of the radiochemical is above 60%.

3.9 Check the specific activity of the radioligand measuring ultraviolet absorbance at 450 nm and the calibration curves established with cold reference compounds. Ensure that the specific activity is greater than 1000 GBq/µmol.

#### 4 [<sup>125</sup>I]R91150 radiotracer synthesis

NOTE: Ensure to follow the same security rules as mentioned in the CLINDE synthesis section.

4.1 Mix 300 µg of R91150 precursor in a solution of 3 µL of absolute ethanol, 3 µL of glacial acetic acid, 15 µL of carrier-free Na<sup>125</sup>I (see **Table of Materials**) (10 mCi) in 0.05 M NaOH and 3 µL of 30% H<sub>2</sub>O<sub>2</sub>. Incubate for 30 min in a glove box.

4.2 Inject the entire reaction into a reverse-phase column (see **Table of Materials**).

4.3 Isolate [<sup>125</sup>I]R91150 by isocratic HPLC run (ACN/water 50/50, 10 mM acetic acid buffer) with a flow rate of 3 mL/min.

4.4 Dilute [<sup>125</sup>I]R91150 in H<sub>2</sub>O for a final volume of 10 mL.

4.5 Inject 10 mL of the diluted reaction onto a concentration column (see **Table of Materials**).

4.6 Elute [<sup>125</sup>I]R91150 from the column with 300 µL of absolute ethanol.

4.7 Evaporate the ethanol by incubating it in a vacuum centrifuge at RT for 40 min.

4.8 Dilute the residue containing [<sup>125</sup>I]R91150 in 300 µL of saline.

4.9 Purify the tracer by HPLC. Determine the elution time using a standard calibration at 450 nm and isolate the single radioactive peak. Establish the radiochemical purity by measuring a single peak in radio TLC. Ensure that the purity of the radiochemical is above 98%.

#### 5 Animal preparation

5.1 Weigh and anesthetize the TgF344-AD rat (male or female, from 2–24 months old) in an induction chamber with 3% isoflurane. Once deeply anesthetized, lower the isoflurane flow to 2% (0.4 L/min, 100% O<sub>2</sub>) in the chamber.

5.2 Position the animal on a pre-warmed bed equipped with an anesthesia nosecone. Maintain isoflurane at 2% (0.4 L/min, 100% O<sub>2</sub>).

5.3 Apply eye gel lubricant in the animal's eyes and confirm the depth of anesthesia via respiratory monitoring; adjust anesthesia if necessary.

5.4 Perform the 24 G catheter insertion in the tail vein.

## 6 SPECT acquisition

6.1 Transfer the animal to the camera bed (**Figure 1E**).

6.2 Secure the head of the animal onto the bite bar and fix the head supports.

6.3 Set up the experiment on a 60 min scan constituting 60 frames of 1 min. Reuse all other parameters set up in step 1. Click on the **Update Image** button to update the animal position.

6.4 Set the scan area by sliding the cursors with the help of the three images in the bottom part of the screen for the three dimensions.

6.5 Inject 500  $\mu$ L of the radioactive radiotracer ( $[^{125}\text{I}]\text{CLINDE}$  or  $[^{125}\text{I}]\text{R91150}$ ), and then flush the tube with 300  $\mu$ L of sterile 0.9% NaCl. Simultaneously click on **Start Acquisition** to start the scan.

6.6 During the scan time, ensure to maintain the animal under constant anesthesia with respiration rate monitoring. Adjust the flow of isoflurane if needed.

6.7 Once the scan is over, quickly euthanize the anesthetized animal by decapitation.

## 7 Scan reconstruction

7.1 Open the scan reconstruction software (see **Table of Materials**), and then open the data set, looking for the [filename].parameters file, created in the folder of the scan.

7.2 Select the isotope of interest. Note that the **Listmode** parameter allows multiple isotope selection at this step.

7.3 Select the following parameters: 0.4 mm Voxel size, 4 (POS-EM) subsets, 6 iterations (24ME-EM equivalent), no post-filter, and the isotope corresponding Decay Correction. Select the output format to NIfTI, and then select **Start SPECT** reconstruction.

## 8 Rat brain extraction

8.1 After decapitation, quickly transfer the head of the animal to the dissection bench.

8.2 With scissors, carefully cut the skin on top of the head from the back to the front till the

middle of the eyes.

8.3 Cut off the excess muscles around the base of the skull and the cervical vertebrae.

8.4 Next, carefully place one blade of the scissors in the hole at the back of the skull, the foramen magnum, and remove the back part of the skull with surgical pliers.

8.5 Then, with surgical pliers, carefully remove the top part of the skull. The skull of old male rats can be thick, remove as small pieces to avoid damage to the brain.

8.6 Carefully cut the meninges with scissors. Meninges can damage the brain during the extraction process; remove it as a precaution.

8.7 After removing the top part of the skull, turn the head of the animal around, and with a small flat spatula, carefully pull the brain out by cutting the optic and trigeminal nerves.

8.8 Carefully transfer the brain onto a flat, clean glass surface for dissection on ice.

8.9 Use a flat metal spatula and a razor blade to dissect the regions of interest of the brain. Place the tissues in a 2 mL centrifuge tube and weigh the tissue obtained. Use the brain section directly for cell isolation or quickly freeze it in liquid nitrogen for later use.

## 9 Cell isolation

9.1 Make sure to work in a clean and sterile environment. Working under a class-II biosafety cabinet (BSC) is advised. Ensure that the gloves and every piece of equipment introduced into the BSC are sterile.

9.2 To prepare the cells for cell sorting, follow the protocol from Jaclyn M. Schwarz<sup>14</sup>.

NOTE: In this experiment, a commercially available Neural dissociation kit (see **Table of Materials**) was used for cell preparation.

9.2.1 Put the samples into a 2 mL centrifuge tube with 1 mL of HBSS (Ca- and Mg-free), and then centrifuge (300 x g, 2 min, room temperature = RT) and remove the supernatant without disturbing the pellet.

9.2.2 Add 1900 µL of enzyme mix-1 and incubate it for 15 min at 37 °C while agitating the tubes by inversion every 5 min.

9.2.3 Add 30 µL of enzyme mix-2, agitate gently with pipette 1 (see **Table of Materials**) back and forth 30 times. Then, incubate for 15 min at 37 °C while agitating the tubes by inversion every 5 min.



9.2.4 Mix gently back and forth with pipette 2, and then pipette 3 before incubating for 10 min at 37 °C to dissociate the tissues.

9.2.5 Filter the cells with an 80 µm cell strainer, add 10 mL of HBSS (Ca- and Mg-free). Centrifuge (300 x *g*, 10 min, RT) and remove the supernatant without disturbing the pellet.

9.2.6 For myelin depletion, resuspend the pellet with 400 µL of myelin removal buffer (see **Table of Materials**), and then add 100 µL of myelin removal beads (see **Table of Materials**), before incubating for 15 min at 4 °C.

9.2.7 Add 5 mL of myelin removal buffer, centrifuge (300 x *g*, 10 min, RT), and remove the supernatant without disturbing the pellet.

9.2.8 Add 500 µL of myelin removal buffer and place the tube into the magnetic field column. Wash the column with 1 mL of myelin removal buffer four times.

9.2.9 Centrifuge (300 x *g*, 2 min, RT) and remove the supernatant without disturbing the pellet. Vortex briefly (2 s) to dissociate the cells and add 5 µL of Fc block CD32. Vortex again and incubate for 5 min at 4 °C.

9.2.10 Add 100 µL of the mix of primary antibodies of interest; incubate for 20 min at 4 °C.

9.2.11 Centrifuge (350 x *g*, 5 min, 4 °C) and remove the supernatant without disturbing the pellet. Blot the tubes upside-down on soft paper.

9.2.12 After a brief vortex (2 s), add 100 µL of the secondary antibody mix and incubate for 15 min at 4 °C.

9.2.13 Add 2 mL of myelin removal buffer, centrifuge (350 x *g*, 5 min, 4 °C) and remove the supernatant without disturbing the pellet. Blot the tubes upside-down on soft paper. Resuspend the cells in 250 µL of sterile PBS and proceed directly to cell sorting.

## 10 Cell sorting

10.1 Prepare the microfuge tube with 500 µL of sterile PBS for collecting the sorted cells.

10.2 Add 10 µL of Hoechst per 1000 µL of cell solution to color the nuclei of the living cells and distinguish them from the dead cells.

10.3 Transfer the cells as soon as possible to the cell sorting machine at 4 °C.

10.4 First, sort the cells by forward and side scatter, and then sort the Hoechst positive cells. Next, sort the cells based on the antibodies of interest. Collect the positively stained cells separately. Make sure to distinguish the positive cells from the autofluorescent ones.

10.5 Count the number of sorted cells for each pool of interest.

## 11 Gamma counting

11.1 Calibrate the  $\gamma$  counting system with 10  $\mu$ L of the same phantom solution used for the SPECT calibration but dilute it in 1 mL of water.

NOTE: The phantom solution is diluted because of the enhanced precision of the  $\gamma$  counting system.

11.2 Place the tube of sorted cells in the  $\gamma$  counting system and proceed with the  $\gamma$  counting according to the manufacturer's protocol.

### REPRESENTATIVE RESULTS:

WT rats experienced *in vivo* SPECT scan with [ $^{125}$ I]CLINDE radiotracer after a unilateral LPS injection (**Figure 2**). This scan (using summed data from images of 45–60 min post radiotracer injection) showed higher binding of [ $^{125}$ I]CLINDE in the site of the LPS injection (**Figure 2A**) than in the contralateral region of the brain (**Figure 2B**). The *ex vivo* samples that underwent FACS-RTT confirmed those results and revealed the presence of a higher number of [ $^{125}$ I]CLINDE binding sites only in microglia, showing that the cellular origin of the [ $^{125}$ I]CLINDE signal in the ipsilateral side of the brain was microglial (**Figure 3A**)<sup>15</sup>.

Using the same [ $^{125}$ I]CLINDE radiotracer, the protocol was then performed on the hippocampus of old TgF344-AD Rats (12- and 24-month-old) and compared with 24-month-old WT. The results demonstrated that the increase in TSPO binding at 12 months in TgF344-AD rats was restricted to astrocytes. In 24-month-old rats, the increase in TSPO binding was due to both astrocytic and microglial alterations (**Figure 3B**). The results showed that the TSPO overexpression in astrocytes is probably observed before the microglial one. Independently, using the radiotracer [ $^{125}$ I]R91150, this technique was used at a cellular scale to show that in older TgF344-AD rats, striatal astrocytes displayed a decreased 5HT<sub>2A</sub>R density when compared with WT (**Figure 3C**)<sup>16</sup>.

Finally, FACS-RTT was performed on human AD post-mortem samples. After dissociation, the cells were incubated with [ $^{125}$ I]CLINDE before staining and the FACS procedure. This allowed discovering a cortical overexpression of TSPO in both astrocytes and microglia of AD subjects compared with age-matched controls (**Figure 3D**).

### FIGURE AND TABLE LEGENDS:

**Figure 1: SPECT Camera Set-up.** (A) SPECT camera overall presentation. (B) Bed presentation with heater and respiratory rate monitoring. (C) Anesthesia tube plugs. (D) Heating bed and respiratory probe socket. (E) Phantom positioning monitoring view from the software.

**Figure 2: TSPO brain imaging using SPECT with [ $^{125}$ I]CLINDE radiotracer.** Representative images (45–60 min post-injection of [ $^{125}$ I]CLINDE) of the hippocampus after (A) LPS or (B) saline injection

in the ipsilateral (white) and contralateral (red) side of the brain. *In vivo* time-activity curves measured in the volume-of-interest are represented in the right panel. SPECT: single-photon emission computed tomography; TSPO: translocator protein; LPS: lipopolysaccharide n = 7 animals per condition. This figure has been modified from Tournier et al.<sup>15</sup>.

**Figure 3: Quantification of TSPO and 5HT<sub>2A</sub>R.** (A) Cellular origin of TSPO overexpression after a unilateral brain injection of LPS. The radioactivity was measured (% injected dose/g of tissue) in each cell population in the contralateral (gray, n = 7) and the ipsilateral (green, n = 7) side of the injection. Statistical test used: paired *t*-test. (B) TSPO in old TgF344-AD rat. The [<sup>125</sup>I]CLINDE concentrations (% injected dose/g of tissue) were determined in 24-month-old wild-type animals (gray, n = 9) and in 12- (green, n = 8) and 24-month-old (purple, n = 7) TgF344-AD rats. Statistical test used: two-way ANOVA. (C) 5HT<sub>2A</sub>R is decreased in astrocytes of the striatum in old TgF344-AD rats. The [<sup>125</sup>I]R91150 concentration was determined in astrocytes and microglia at the cellular level (% injected dose/cell) in WT (gray, n = 7) and old TgF344-AD (green, n = 11) rats. Statistical test used: one-way ANOVA. (D) Cell provenance of TSPO overexpression in the frontal cortex in Alzheimer's disease (AD). In each cell population, the radioactivity is measured (% injected dose/g of tissue) in AD subjects (green, n = 9) and control (gray, n = 9). Statistical test used: unpaired *t*-test. All data are represented as mean ± 95% CI with the following annotation: \* *p* < 0.05, \*\* *p* < 0.01, \*\*\* *p* < 0.001.

## DISCUSSION:

To our knowledge, this technique was the first to describe an approach that allows a better understanding of *in vivo* binding alterations of a radiotracer at the cellular level. The protocol describes a multiscale method to quantify radiotracer binding at the cellular level using [<sup>125</sup>I]CLINDE (TSPO) or [<sup>125</sup>I]R91150 (5HT<sub>2A</sub>R) as examples.

This technique is robust and sensitive enough to precisely detect the cellular origin of a wide spectrum of glial cell alterations ranging from an intense inflammatory reaction induced by LPS to more subtle glial cell alterations observed in a rat model of AD, bringing important complementary information to *in vivo* nuclear neuroimaging, as the microglial origin of the signal obtained with SPECT that was determined. The study further showed that FACS-RTT was even able to discern neuroreceptor density alterations at the cellular scale with the example of 5HT<sub>2A</sub>R (Figure 3C). Finally, evidence for using the technique in human post-mortem tissues was provided, showing an increased TSPO concentration in astrocytes and microglia of AD subjects.

The main advantage of this technique is its complementarity with PET and SPECT imaging. Indeed, nuclear imaging is a powerful technique that can extract information from a brain region or voxel level. However, its limit resides at the cellular scale; it is impossible to distinguish each cell type's contribution to the signal. FACS-RTT allows going further by revealing a radiotracer concentration in each cell type. Interestingly, in theory, an unlimited set of targets can be assessed with this technique, the limitation being the availability of a radiotracer for the target of interest.

The critical steps of the protocol include the use of radioactivity that must be performed in a secure environment with qualified personnel. Furthermore, it is crucial to consider radioactive

decay. For FACS preparation, one must ensure antibody specificity, wavelength, light intensity that differ depending on the cell type and need optimization for efficient cell sorting.

One of the limitations of this technique underlined in the studies presented here lies in using aged animals and human post-mortem brain samples because of autofluorescent cells. Lipofuscin, i.e., a residue of lysosomal digestion, is fluorescent and accumulates in aging neurons, microglia, and astrocytes. FACS can, with prior optimization, distinguish autofluorescent cells from positively labeled ones, which is an essential step if older animals are studied. Another limitation of the technique is the impossibility to directly compare the radiotracer concentration between the different sorted cell types across different animals. This could be performed if the concentration of the non-metabolized, non-protein bound radiotracers in blood was considered for normalization across animals.

One final limitation is the need for all the equipment used, e.g., cyclotron, PET/SPECT camera, FACS, and  $\gamma$  counter, to be in close physical proximity to each other, especially if short half-life isotopes are used for *in vivo* imaging and FACS-RTT.

FACS-RTT could also be used as a standalone approach, i.e., not necessarily following an *in vivo* nuclear imaging study<sup>15</sup>. The complexity of brain disease requires studying mechanisms at a cellular level or single-cell scale. FACS-RTT could be a translational tool bridging *in vivo* imaging approaches with a vast spectrum of *ex vivo* or *in vitro* cellular and molecular biology approaches.

#### ACKNOWLEDGMENTS:

This work was supported by the Swiss National Science Foundation (grant no. 320030-184713). Authors BBT and KC are supported by the Velux Foundation (project n. 1123). Author ST received support from the Swiss National Science Foundation (Early Post-Doc Mobility Scholarship, no. P2GEP3\_191446), the Prof Dr. Max Cloetta Foundation (Clinical Medicine Plus scholarship), and the Jean and Madeleine Vachoux Foundation.

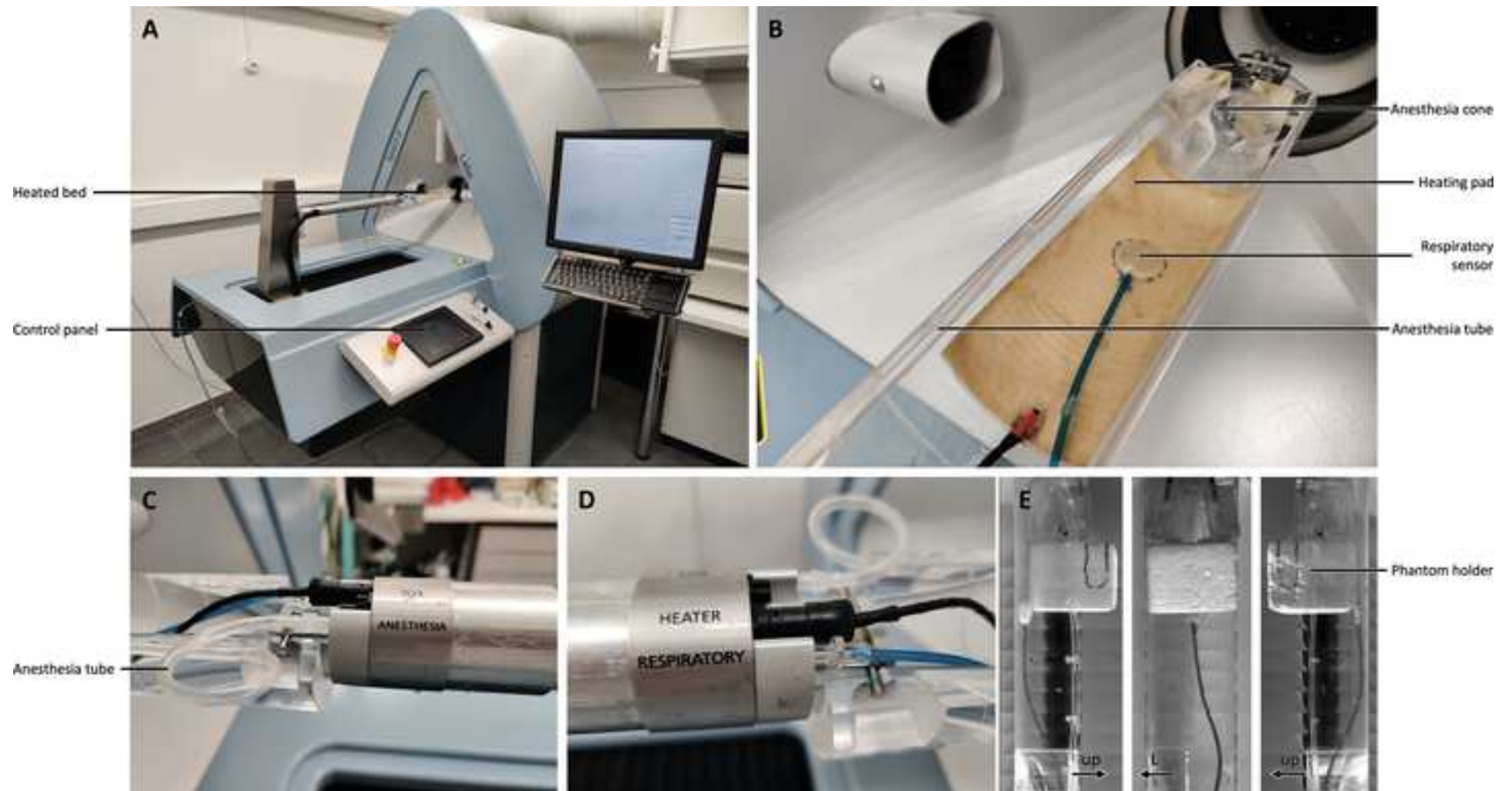
#### DISCLOSURES:

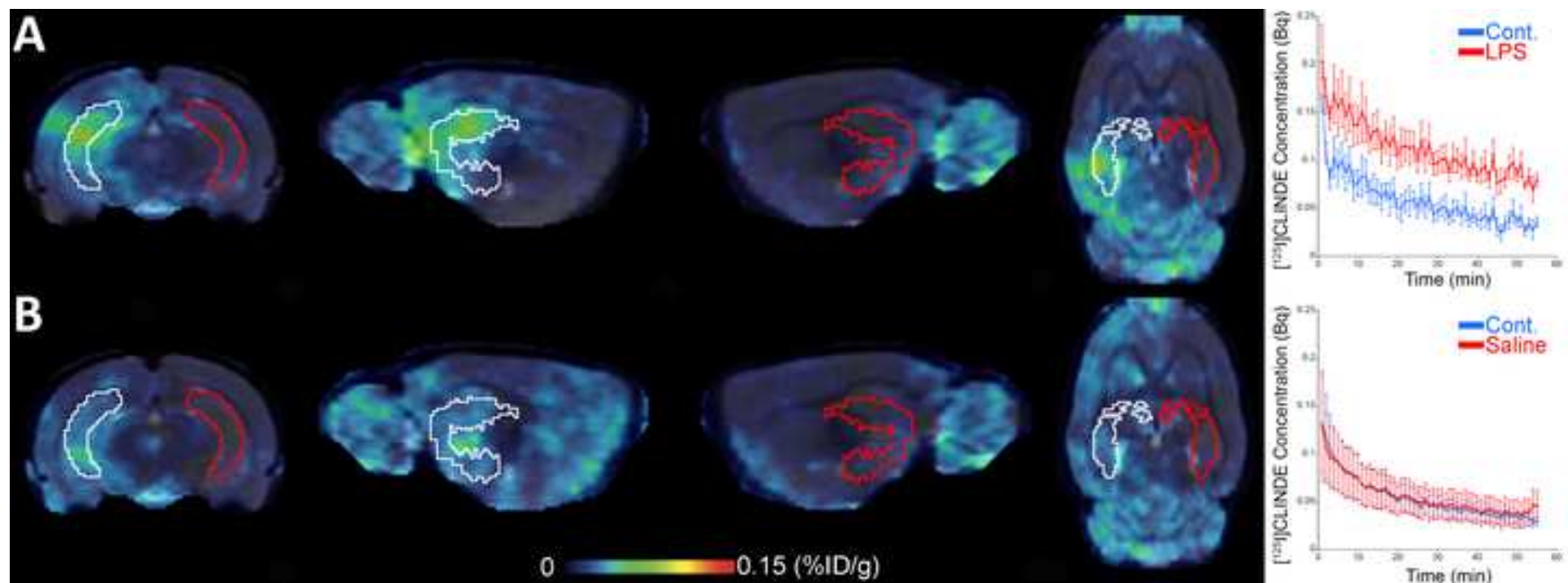
The authors declare no conflicts of interest.

#### REFERENCES:

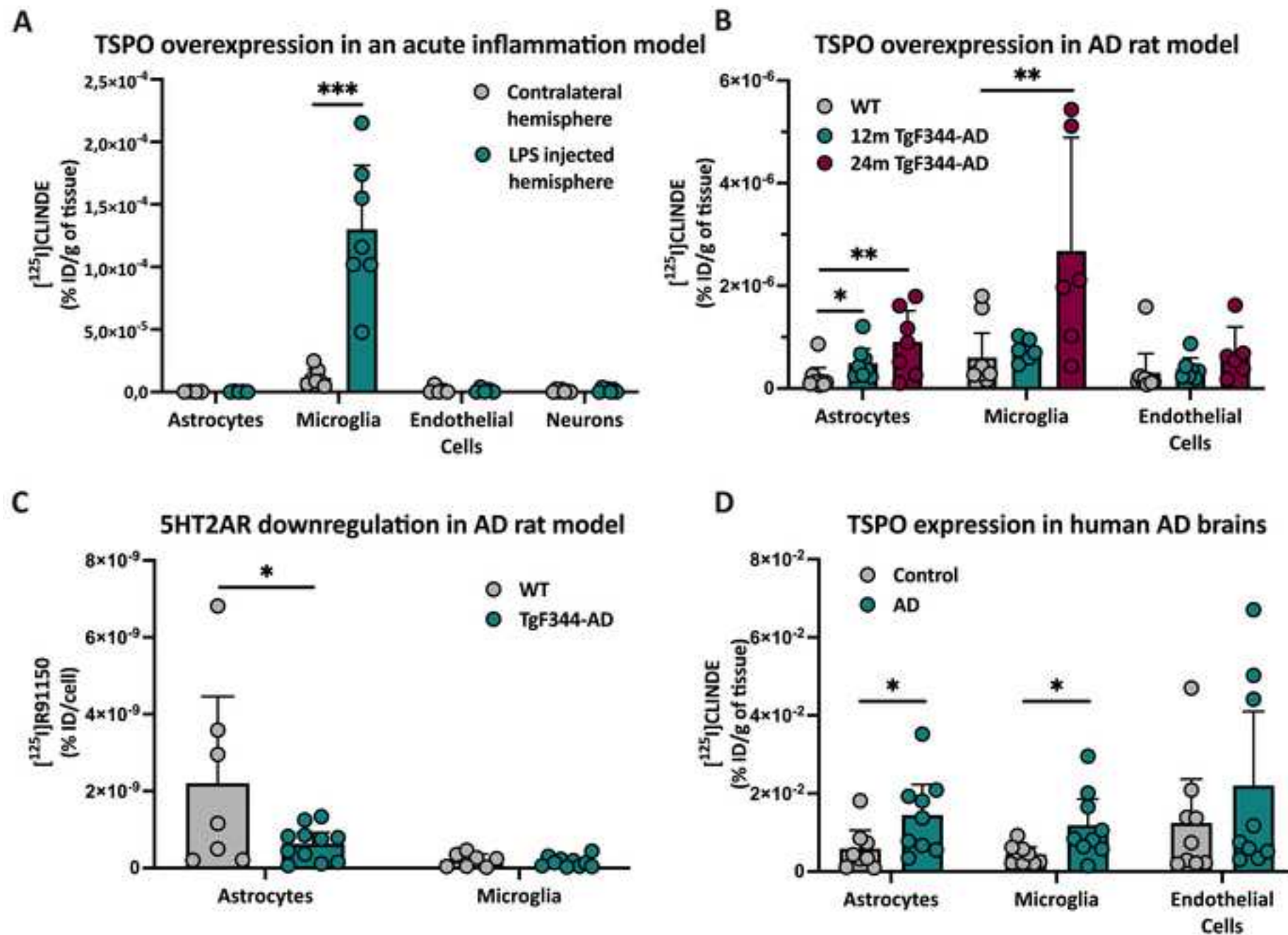
1. Nichols, E. et al. Global, regional, and national burden of Alzheimer's disease and other dementias, 1990–2016: a systematic analysis for the Global Burden of Disease Study 2016. *The Lancet Neurology*. **18** (1), 88–106 (2019).
2. Kinney, J. W. et al. Inflammation as a central mechanism in Alzheimer's disease. *Alzheimer's & Dementia (New York, N. Y.)*. **4**, 575–590 (2018).
3. D'Amelio, M., Puglisi-Allegra, S., Mercuri, N. The role of dopaminergic midbrain in Alzheimer's disease: Translating basic science into clinical practice. *Pharmacological Research*. **130**, 414–419 (2018).
4. D'Amelio, M., Serra, L., Bozzali, M. Ventral tegmental area in prodromal Alzheimer's disease: Bridging the gap between mice and humans. *Journal of Alzheimer's Disease: JAD*. **63** (1), 181–183 (2018).

5. Cohen, R. M. et al. A transgenic Alzheimer rat with plaques, tau pathology, behavioral impairment, oligomeric  $\alpha\beta$ , and frank neuronal loss. *The Journal of Neuroscience: The Official Journal of the Society for Neuroscience*. **33** (15), 6245–6256 (2013).
6. Morrone, C. D. et al. Regional differences in Alzheimer's disease pathology confound behavioural rescue after amyloid- $\beta$  attenuation. *Brain: A Journal of Neurology*. **143** (1), 359–373 (2020).
7. Berkowitz, L. E., Harvey, R. E., Drake, E., Thompson, S. M., Clark, B. J. Progressive impairment of directional and spatially precise trajectories by TgF344-Alzheimer's disease rats in the Morris Water Task. *Scientific Reports*. **8** (1), 16153 (2018).
8. Koulousakis, P., van den Hove, D., Visser-Vandewalle, V., Sesia, T. Cognitive improvements after intermittent deep brain stimulation of the nucleus basalis of meynert in a transgenic rat model for Alzheimer's disease: A preliminary approach. *Journal of Alzheimer's Disease: JAD*. **73** (2), 461–466 (2020).
9. Tournier, B. B. et al. Spatial reference learning deficits in absence of dysfunctional working memory in the TgF344-AD rat model of Alzheimer's disease. *Genes, Brain, and Behavior*. e12712 (2020).
10. Tournier, B. B., Tsartsalis, S., Ceyzériat, K., Garibotto, V., Millet, P. In vivo TSPO signal and neuroinflammation in Alzheimer's disease. *Cells*. **9** (9) (2020).
11. Backes, H. [11C]raclopride and extrastriatal binding to D2/3 receptors. *NeuroImage*. **207**, 116346 (2020).
12. Millet, P. et al. Quantification of dopamine D(2/3) receptors in rat brain using factor analysis corrected [18F]Fallypride images. *NeuroImage*. **62** (3), 1455–1468 (2012).
13. Tsartsalis, S. et al. A modified simplified reference tissue model for the quantification of dopamine D2/3 receptors with [18F]Fallypride images. *Molecular Imaging*. **13** (8), 7290.2014.00028 (2014).
14. Schwarz, J. M. Using fluorescence-activated cell sorting to examine cell-type-specific gene expression in rat brain tissue. *Journal of Visualized Experiments: JoVE*. **99**, e52537 (2015).
15. Tournier, B. B. et al. Fluorescence-activated cell sorting to reveal the cell origin of radioligand binding. *Journal of Cerebral Blood Flow & Metabolism*. **40** (6), 1242–1255 (2020).
16. Tournier, B. B. et al. Astrocytic TSPO upregulation appears before microglial TSPO in Alzheimer's disease. *Journal of Alzheimer's Disease: JAD*. **77** (3), 1043–1056 (2020).















Click here to access/download  
**Table of Materials**  
Table of Materials-62883\_R2.xls



We would like to thank the editors for their second constructive reviews. The changes are expressed in the manuscript in blue.

### **Editorial comments:**

1. Please note that the manuscript was formatted to fit the journal standard. Comments to be addressed are included in the manuscript.

Thank you for this mention, we will answer those comments in the following for clarity.

2. The highlighted protocol steps exceed the 3-page limit (~3.5 pages). Please reduce the highlighting to fit the 3-page limit to follow the journal standard. Consider merging some shorter steps to fit the page limit of highlighting. We have reduced the highlighted protocol steps by merging some shorter steps together. The following steps have been merged (the former step numbers are used here):

- Steps 1.2 and 1.3 → Step 1.2
- Steps 1.4 and 1.5 → Step 1.3
- Steps 3.3 and 3.4 → Step 3.3
- Steps 3.5 and 3.6 → Step 3.4
- Steps 3.7 and 3.8 → Step 3.5
- Steps 6.3 and 6.4 → Step 6.3
- Steps 8.9 and 8.10 → Step 8.9
- Steps 9.3.3 and 9.3.4 → Step 9.3.3
- Steps 9.3.10 and 9.3.11 → Step 9.3.9
- Steps 9.3.15 and 9.3.16 → Step 9.3.13

3. Explicit permission for the use of previously published figures can be expressed in the form of a letter from the editor or a link to the editorial policy that allows re-prints. Please upload this information as a .doc or .docx file to your Editorial Manager account.

We have added .docx documents with link and information about reuse policy of SAGE journal from which 1 figure have been reused.

4. Please ensure that all relevant essential supplies, reagents, and equipment are included in the Table of Materials.

We have updated the Table of Materials with all the missing supplies that were cited in the manuscript.

5. Comments included in the manuscript:

- (Line 211, now 222): to what volume/concentration?

The volume of 300 µL of saline has been added in the manuscript.

- (Lines 219 – 221, now 230 – 232): Please specify the strain, sex, age of the rats used in this study.

The strain, sex and age of the rats has been added.

- (Lines 282 – 283, now 296 – 297): Please rephrase the sentence to add more clarity.

The phrase has been rephrased to add more clarity to this step.

- (Line 316, now 327): Pipette 1? There is nothing specific to pipette 1 in the Table of Materials. Please ensure that all the necessary details are included (size, volume etc.)

The mention to the “pipette 1” has been added in the Table of Materials.

- (Lines 321 – 322, now 339 – 340): Pipette 2 and 3? There is nothing specific to these in the Table of Materials. Please specify the (size, volume etc.). If it was performed using any commercial Dissociator, please specify in the Table of Materials.

The mentions to the “pipette 2” and “pipette 3” have been added in the Table of Materials.

- (Line 327, now 345): Please include this in the Table of Materials. Is this a component in the myelin removal beads II?

Yes, it is a component of the myelin removal beads II kit. This detail has been added in the Table of Materials.

- (Lines 374 – 375, now 395 – 397): How much diluted? what is used for dilution?

The details about the dilution have been added in the manuscript.

- (Line 377, now 399 – 400): Is it performed according to the manufacturer's protocol. If so, please mention it in the step.

Yes it is performed according to the manufacturer's protocol, we have added this mention in the manuscript.



**Fluorescence-activated cell sorting to reveal the cell origin of radioligand binding**

**Author:**

Benjamin B Tournier, Stergios Tsartsalis, Kelly Ceyzériat, et al

**Publication:**

Journal of Cerebral Blood Flow & Metabolism

**Publisher:**

SAGE Publications

**Date:**

06/01/2020

**Gratis Reuse**

If you are a SAGE journal author requesting permission to reuse material from your journal article, please note you may be able to reuse your content without requiring permission from SAGE. Please review SAGE's author re-use and archiving policies at <https://us.sagepub.com/en-us/nam/journal-author-archiving-policies-and-re-use> for more information.

If your request does not fall within SAGE's reuse guidelines, please proceed with submitting your request by selecting one of the other reuse categories that describes your use. Please note, a fee may be charged for reuse of content requiring permission. Please submit a ticket through the [SAGE Permissions Portal](#) if you have questions.